Oxidative Damage Linked to Neurodegeneration by Selective α-Synuclein Nitration in Synucleinopathy Lesions

Benoit I. Giasson,[1]* John E. Duda,[1]* Ian V. J. Murray,[1] Qiping Chen,[3] José M. Souza,[3] Howard I. Hurtig,[2] Harry Ischiropoulos,[3] John Q. Trojanowski,[1] Virginia M.-Y. Lee[1]†

Aggregated α-synuclein proteins form brain lesions that are hallmarks of neurodegenerative synucleinopathies, and oxidative stress has been implicated in the pathogenesis of some of these disorders. Using antibodies to specific nitrated tyrosine residues in α-synuclein, we demonstrate extensive and widespread accumulations of nitrated α-synuclein in the signature inclusions of Parkinson's disease, dementia with Lewy bodies, the Lewy body variant of Alzheimer's disease, and multiple system atrophy brains. We also show that nitrated α-synuclein is present in the major filamentous building blocks of these inclusions, as well as in the insoluble fractions of affected brain regions of synucleinopathies. The selective and specific nitration of α-synuclein in these disorders provides evidence to directly link oxidative and nitrative damage to the onset and progression of neurodegenerative synucleinopathies.

Oxidative injury has been implicated in the pathogenesis of neurodegenerative disorders including Alzheimer's disease (AD) (*1*), Parkinson's disease (PD) (*2*, *3*), dementia with Lewy bodies (DLB) (*4*), amyotrophic lateral sclerosis (*5*), and Huntington's disease (*6*). Oxidative injury occurs when the compensatory antioxidant capacity of cells is overwhelmed by excess production of reactive species that damage lipids, nucleic acids, proteins, and other cellular components. Both reactive oxygen and nitrogen species are produced in vivo and may act synergistically to form nitrating agents that modify proteins as well as other biomolecules such as thiols, aldehydes, and lipids (*7*, *8*). For example, superoxide reacts with nitric oxide to generate peroxynitrite that forms biologically active nitrating agents in the presence of CO_2 or other catalysts (redox active metals, or metalloproteins) (*9*, *10*), which can convert native tyrosine residues in proteins into 3-nitrotyrosine (3-NT).

Initially described over 10 years ago (*11*), α-synuclein (α-syn) is a 140–amino acid, highly conserved protein that is abundant in neurons, especially presynaptic terminals (*12*, *13*). Two mutations in the α-syn gene have been shown to be pathogenic for familial PD in rare kindreds (*14*, *15*), and it has been demonstrated that α-syn is the major component of Lewy bodies (LBs) and Lewy neurites (LNs) in PD, DLB, and the LB variant of AD (LBVAD) (*16*–*18*). Moreover, α-syn also appears to be a major component of glial and neuronal cytoplasmic inclusions (GCIs and NCIs) in multiple system atrophy (MSA) brains (*19*, *20*), as well as of the LB-like inclusions, neuraxonal spheroids, and LNs in neurodegeneration with brain iron accumulation type 1 (NBIA1), a rare disorder previously termed Hallervorden-Spatz disease (*19*, *21*).

Immunoreactive 3-NT was detected in LBs of the PD brain and appears to be a common feature of α-syn lesions in many synucleinopathies (*22*), but no protein building blocks of disease-specific lesions that are modified with 3-NT have been identified in any neurodegenerative disorder. Thus, to determine if α-syn in the hallmark lesions of synucleinopathies are specifically nitrated, we raised monoclonal antibodies (mAbs) to nitrated α-syn (*23*) and screened them by enzyme-linked immunosorbent assay (ELISA) to identify anti–nitrated α-syn mAbs using nitrated and unmodified α-syn as well as other nitrated proteins, i.e., recombinant human β-syn, ribonuclease A (RNase A), cytochrome c, bovine superoxide dismutase–1 (SOD-1), and phospholipase A_2 (PLA_2). Several mAbs (e.g., nSyn 8, 14, and 24) specifically recognized nitrated α- and β-syn but not nonnitrated α-syn or any other nitrated proteins tested (Fig. 1A). mAb nSyn 12 reacted with nitrated α-syn, as well as with nitrated β-syn, RNase A, and PLA_2, but not with nonnitrated α-syn. Western blots were used to further characterize mAbs that recognized nitrated synucleins by ELISA, and nSyn 24 bound specifically to nitrated α- and β-syn, but not to nonnitrated α-syn or other nitrated proteins (Fig. 1B). Indeed, nSyn 24 did not cross-react with these other proteins even after longer Western blot exposure times. However, nSyn 24 also recognized dimerized nitrated α-syn with an apparent molecular mass of about 35 kD (Fig. 1B). In contrast, anti–α-syn mAb LB509 (*18*) recognized nitrated and nonnitrated α-syn, whereas polyclonal anti–3-NT (*24*) recognized all the nitrated proteins tested. However, because the cytochrome c and PLA_2 immunoreactive bands were weak, these proteins may be nitrated to a lesser extent, or the antibody may have less affinity for 3-NT in these proteins.

The epitopes recognized by the anti–nitrated α/β-syn mAbs were characterized by Western blot performed on nitrated full-length and truncated recombinant human α-syn proteins, as well as on nitrated recombinant α-syn proteins that were mutagenized to substitute Phe for one or more of the four Tyr (Y) residues in human α-syn (i.e., Y39, Y125, Y133, and/or Y136). These studies showed that mAbs nSyn 8, nSyn 12, and nSyn 24 recognized the COOH-terminal region of α-syn because none recognized nitrated α-syn amino acids 1 to 110 or 1 to 120; however, the substitution of any single Tyr residue with Phe was not sufficient to abolish the binding of these antibodies to nitrated α-syn (Fig. 1C) (*25*). The binding of nSyn 12 was dependent on nitration of either Y125 or Y136, but the recognition of nitrated Y136 dominated that of nitrated Y125 (Fig. 1C). The epitope recognized by nSyn 24 also was dependent on nitration of two Tyr residues, and Y133 appeared to be the dominant protein, with the reactivity for nitrated Y133 being more robust than nitrated Y125. The epitope recognition of nSyn 14 is dependent on the nitration of Y39 in α-syn or β-syn (Fig. 1C). The conservation of all four Tyr residues and the amino acid sequences proximal to them in human α- and β-syn may explain the recognition of both nitrated synuclein proteins by all the mAbs reported here, as verified by Western blot analysis and ELISA.

In immunohistochemical studies, numerous LBs, LNs, GCIs, NCIs, LB-like inclusions, and neuraxonal spheroids in brains with different synucleinopathies were robustly labeled by the mAbs nSyn 8, 12, and 24, which recognize the nitrated COOH-terminal region of α-syn (Fig. 2). For example, in DLB and LBVAD brains, staining with nSyn 8 detected abundant cortical and nigral LBs (Fig. 2, A to C), but LNs were not as extensively labeled, whereas many GCIs and occasional NCIs were detected by this mAb in MSA brains (Fig. 2D). Further, many LB-like

[1]Center for Neurodegenerative Disease Research and Department of Pathology and Laboratory Medicine, [2]Department of Neurology, University of Pennsylvania, Philadelphia, PA 19104, USA. [3]Stokes Research Institute and Department of Biochemistry and Biophysics, Children's Hospital of Philadelphia and University of Pennsylvania, Philadelphia, PA 19104, USA.

*These authors contributed equally to this work.
†To whom correspondence should be addressed. E-mail: vmylee@mail.med.upenn.edu

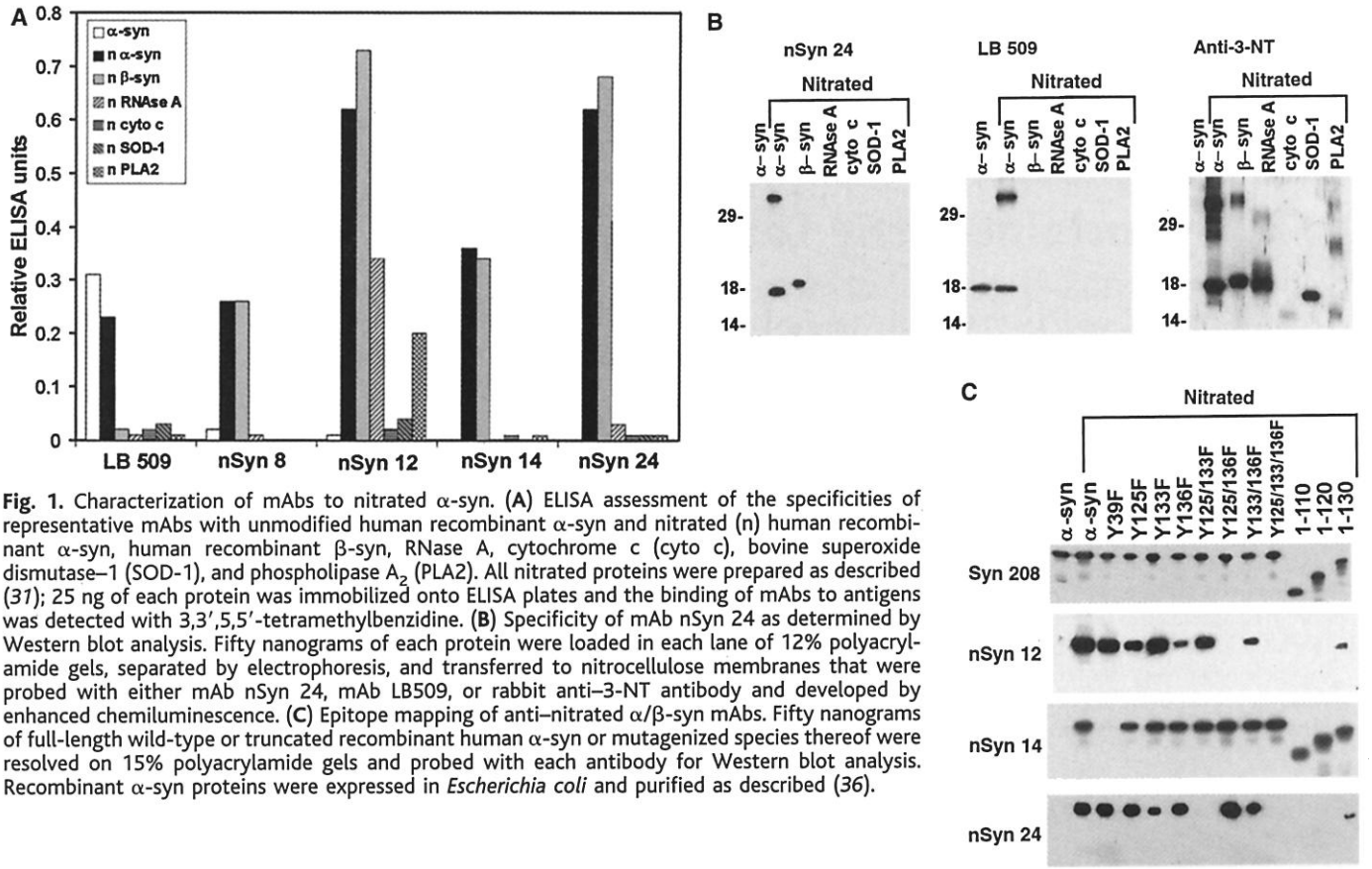

Fig. 1. Characterization of mAbs to nitrated α-syn. (**A**) ELISA assessment of the specificities of representative mAbs with unmodified human recombinant α-syn and nitrated (n) human recombinant α-syn, human recombinant β-syn, RNase A, cytochrome c (cyto c), bovine superoxide dismutase–1 (SOD-1), and phospholipase A_2 (PLA2). All nitrated proteins were prepared as described (*31*); 25 ng of each protein was immobilized onto ELISA plates and the binding of mAbs to antigens was detected with 3,3′,5,5′-tetramethylbenzidine. (**B**) Specificity of mAb nSyn 24 as determined by Western blot analysis. Fifty nanograms of each protein were loaded in each lane of 12% polyacrylamide gels, separated by electrophoresis, and transferred to nitrocellulose membranes that were probed with either mAb nSyn 24, mAb LB509, or rabbit anti–3-NT antibody and developed by enhanced chemiluminescence. (**C**) Epitope mapping of anti–nitrated α/β-syn mAbs. Fifty nanograms of full-length wild-type or truncated recombinant human α-syn or mutagenized species thereof were resolved on 15% polyacrylamide gels and probed with each antibody for Western blot analysis. Recombinant α-syn proteins were expressed in *Escherichia coli* and purified as described (*36*).

inclusions and neuraxonal spheroids, as well as occasional GCIs, were detected by nSyn 8 in the NBIA1 brain (Fig. 2E). Similarly, the nSyn 12 mAb labeled large numbers of LBs (Fig. 2F) and GCIs (Fig. 2G) in DLB and MSA brains, respectively. The nSyn 24 mAb robustly stained cortical and nigral LBs, LNs, and neuraxonal spheroids in PD and DLB brains (Fig. 2, K to O), GCIs in MSA brains (Fig. 2, P and Q), and LB-like inclusions and neuraxonal spheroids in the NBIA1 brain (Fig. 2R). In addition, staining with the nSyn 14 mAb detected nigral LBs (Fig. 2H), and cortical LBs (Fig. 2I) in LBVAD and GCIs in MSA (Fig. 2J), although not as robustly as the antibodies directed against COOH-terminal epitopes. Because the nSyn 8, nSyn 14, and nSyn 24 mAbs detect nitrated α- or β-syn and previous studies demonstrated α-syn but not β-syn in the lesions mentioned above (*16–20*, *26*), we conclude that these mAbs detect only nitrated α-syn in these lesions. Staining with the mAbs labeled the peripheral region more intensely than the central core of classical LBs. In sharp contrast, none of these mAbs stained AD amyloid plaques, neurofibrillary tangles (NFTs), or any lesions in progressive supranuclear palsy, corticobasal degeneration, or Pick's disease brains (Fig. 2S) (*27*). As an additional control for antibody specificity, nSyn 24 was preincubated with 5 μg of either an unnitrated or nitrated synthetic polypeptide corresponding to amino acids 115 to 140 of human α-syn. Preincubation with the nitrated peptide almost completely eliminated staining (Fig. 2T), compared with antibody absorbed with the unnitrated peptide (Fig. 2U). Collectively, these studies show that nitration of α-syn in synucleinopathies occurs at both the Tyr residues within the COOH-terminal region and at Y39 located within the KTKEGV repeat region.

Using double-label immunofluorescence, we analyzed the abundance of α-syn lesions detected with anti–nitrated α/β-syn mAbs—for example, white-matter GCIs in MSA cerebellum were double-labeled with nSyn 24 and anti–α-syn rabbit antibody SNL 4 (*28*), which was subsequently visualized separately (Fig. 3, A and B) or simultaneously (Fig. 3C). Cortical LBs also were double-labeled with these antibodies (Fig. 3D). Because more extensive analysis revealed that most LBs, GCIs, and spheroids were labeled by both antibodies, nitrated α-syn is a widespread and abundant component of these lesions.

Immunoelectron microscopy revealed that the nSyn 24 mAb labeled filamentous structures in the major α-syn lesions (Fig. 4). For example, nSyn 24 intensely labeled most filaments in the GCIs of MSA (Fig. 4A). Moreover, although nSyn 24 labeled filaments more intensely in the periphery than in the core of LB-like inclusions in NBIA1 (Fig. 4B), cortical LBs (*25*), spheroidlike inclusions (Fig. 4C), and LN-like inclusions in NBIA1 (Fig. 4D) were labeled throughout. The immunolabeling of these lesions was restricted to tubular, filamentous profiles and rare straight filamentous structures (Fig. 4D, inset). Thus, nitrated α-syn is an integral component of the α-syn filaments that form the defining lesions of diverse synucleinopathies.

Because previous studies showed that normal α-syn isolated from control brains is soluble in high-salt (HS) and Triton X-100 buffers, but abnormal forms of α-syn are recovered from HS/Triton X-100–insoluble fractions of synucleinopathy brains (*18*, *19*, *29*), we examined whether nitrated α-syn was present in soluble and insoluble extracts of LBVAD and control brains. In Western blot studies with the nSyn 24 mAb to detect nitrated α-syn, an immunoreactive band with the same electrophoretic mobility as α-syn was present in the HS/Triton-insoluble fraction of the LBVAD brains, but not in control brain or in any of the HS-soluble fractions (Fig. 5). We confirmed and extended these findings by using an anti–α-syn mAb Syn 208 (*28*) to demonstrate α-syn in the HS-soluble fractions of control and LBVAD brains as well as monomeric and aggregated α-syn in the HS/Triton-insoluble fractions of the LBVAD brain (Fig. 5). Further, an antibody specific for β-syn (Syn 207) (*19*, *28*) detected β-syn in the HS fraction of LBVAD

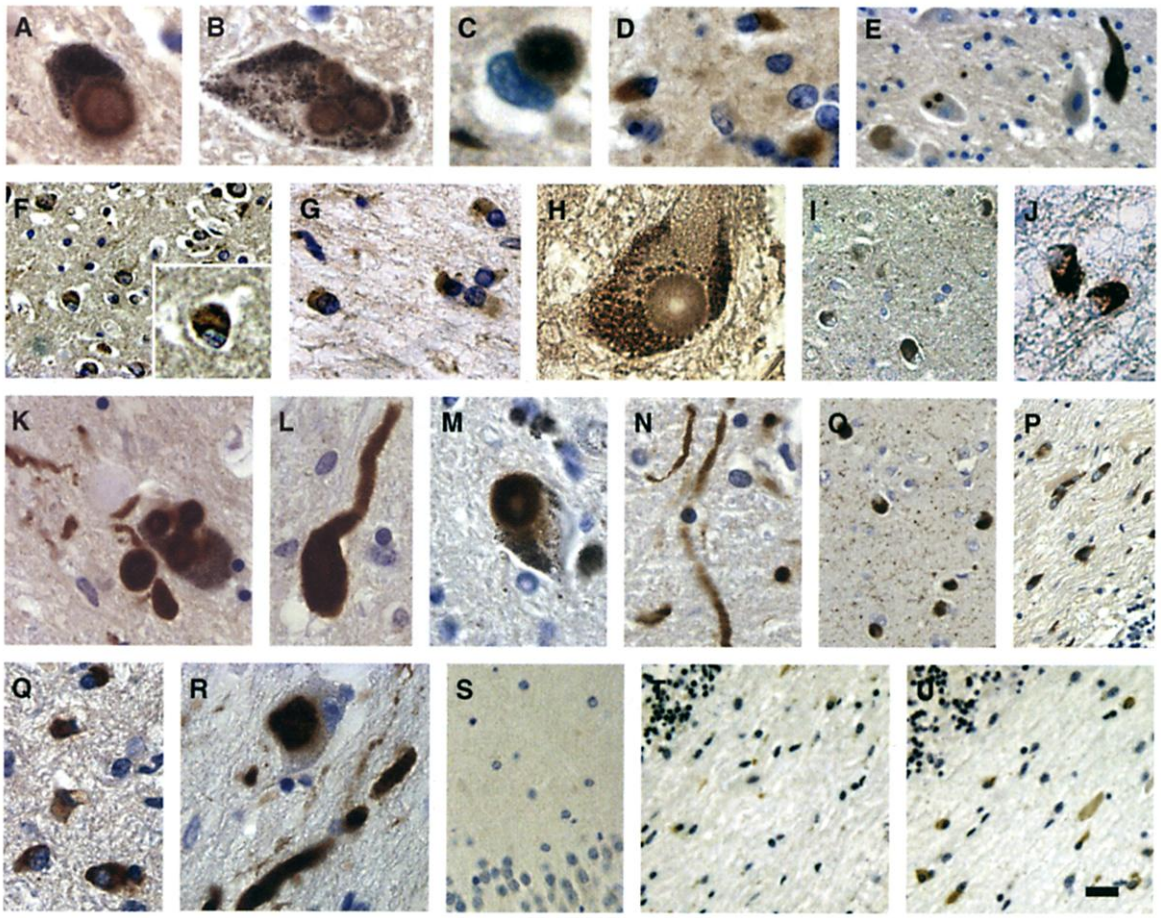

Fig. 2. Immunostaining of diverse synucleinopathy lesions with anti–nitrated α/β-syn mAbs as described (*37*). Immunostaining by the nSyn 8 mAb of nigral LBs in DLB (**A**) and LBVAD (**B**), cortical LBs in LBVAD (**C**), GCIs and NCIs in MSA (**D**), and LBs and neuraxonal spheroids of NBIA1 (**E**). Staining with the nSyn 12 mAb labels cortical LBs in DLB (**F**, with high power view in inset), as well as GCIs in MSA (**G**). Staining with the nSyn 14 mAb labels nigral LBs (**H**), and cortical LBs (**I**), in LBVAD and GCIs in MSA (**J**). Immunostaining with the nSyn 24 mAb labels LBs and LNs (**K**) and a neuraxonal spheroid (**L**) in PD, and nigral LBs (**M**), hippocampal CA2/3 LNs (**N**), and cortical LBs (**O**) in DLB. nSyn 24 also labels GCIs in MSA (**P** and **Q**) and LB-like inclusions and neuraxonal spheroids in NBIA1 (**R**). Staining of AD hippocampus with nSyn 24 reveals no immunoreactivity (**S**), and preabsorption of nSyn 24 with nitrated α-syn COOH-terminal peptide (amino acids 115 to 140) substantially reduced immunostaining (**T**) compared to absorption with nonnitrated peptide (**U**). Bar, 10 μm (A to D, F inset, G, H, J to N, Q, and R) and 30 μm (E, F, I, O, P, and S to U).

and normal control brains, but not in HS/Triton-insoluble fractions (*30*). The higher molecular mass α-syn immunoreactive bands detected with the Syn 208 antibody were not apparent in blots probed with nSyn 24, and we speculate that these bands are dityrosine–cross-linked α-syn polymers (*31*).

The experiments described here provide evidence that α-syn is a specific target of nitrating agents in several diverse neurodegenerative synucleinopathies. We demonstrated this by showing that mAbs specific for nitrated α/β-syn (i) stain numerous LBs, LNs, GCIs, NCIs, LB-like inclusions, and neuraxonal spheroids in synucleinopathies but not in NFTs or senile plaques; (ii) label the filamentous α-syn structures that form these lesions; and (iii) detect nitrated α-syn only in HS/Triton-insoluble fractions of LBVAD brain tissue. Although these mAbs recognized both nitrated α-syn and β-syn, previous observations have shown that β-syn does not accumulate in these lesions (*16–20*, *26*). Thus, our study provides evidence that nitrated α-syn is present in these lesions. Because previous studies only used antibodies specific for 3-NT to detect 3-NT immunoreactivity in NFTs in AD and LBs in PD brains (*22*, *32*, *33*), the exact molecular target of tyrosine nitration in these pathological lesions had not been identified. However, by using the mAbs specific for nitrated α/β-syn described here, we demonstrated that α-syn is indeed a target of nitration in the hallmark lesions of diverse synucleinopathies.

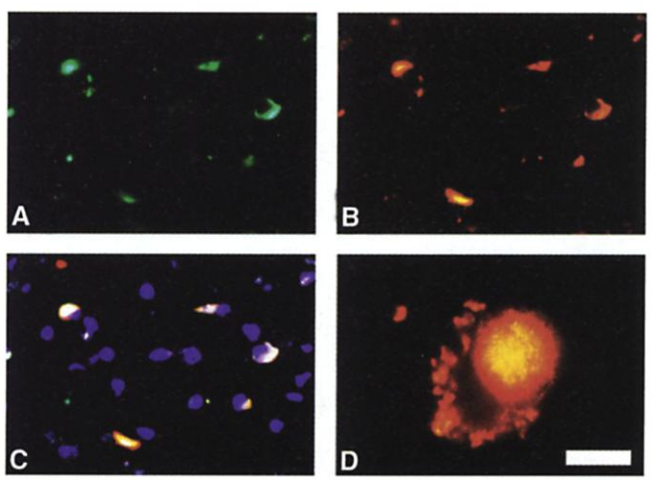

Fig. 3. Double-label immunofluorescence of GCIs with the SNL 4 and nSyn 24 antibodies. Detection of GCIs from MSA with the mouse anti–nitrated α/β-syn mAb nSyn 24 (**A**), affinity-purified rabbit anti–α-syn antibody SNL 4 (**B**), or both (**C**) with a goat anti-mouse immunoglobulin G (IgG) Alexa Fluro 488–conjugated antibody and a goat anti-rabbit IgG Alexa Fluro 594–conjugated antibody (Molecular Probes, Eugene, Oregon). The sections were covered with Vectashield-DAPI (4′,6′-diamidino-2-phenylindole) mounting medium (Vector Laboratories, Burlingame, California). Most GCIs are double-labeled. (**D**) Double-label immunofluorescence demonstrating colocalization of SNL 4 and nSyn 24 immunoreactivities in a cortical LB. Bar, 30 μm (A to C) and 10 μm (D).

Our observation that nitrated α-syn is present only in the HS/Triton-insoluble fractions of LBVAD cortex suggests that the solubility of α-syn may be reduced by tyrosine nitration and that this modification may promote the fibrillogenesis of α-syn and/or its aggregation into hallmark lesions of synucleinopathies. Alternatively, nitration of

α-syn may occur only after it has assembled into filamentous structures. Nitration may render α-syn more resistant to proteolysis or alter other properties of this synaptic protein, thereby playing a mechanistic role in the formation and/or stability of α-syn lesions, as well as in the onset and progression of synucleinopathies.

Although we detected nitrated α-syn in the major signature lesions of diverse synucleinopathies, the extent of this nitration remains to be determined. Further, because nitrating agents also can oxidize tyrosine residues to form *o-o'*-dityrosine, and this can result in the covalent cross-linking of α-syn and the formation of stable α-syn polymers (*31*), more than one nitrating process may contribute to the pathogenesis of α-syn lesions. Because the formation of 3-NT and *o-o'*-dityrosine can occur simultaneously under oxidative and nitrative conditions, species of α-syn that have been modified by *o-o'*-dityrosine cross-linking as well as by 3-NT modification may contribute to the pathogenesis of synucleinopathies.

Our findings suggest that impairment of cellular antioxidative mechanisms or overproduction of reactive species may be a primary event leading to the onset and progression of neurodegenerative synucleinopathies. Thus, elucidation of the role of oxidative and nitrative injury in mechanisms underlying these and other neurodegenerative disorders may lead to the identification of therapeutic targets to prevent or reverse these diseases.

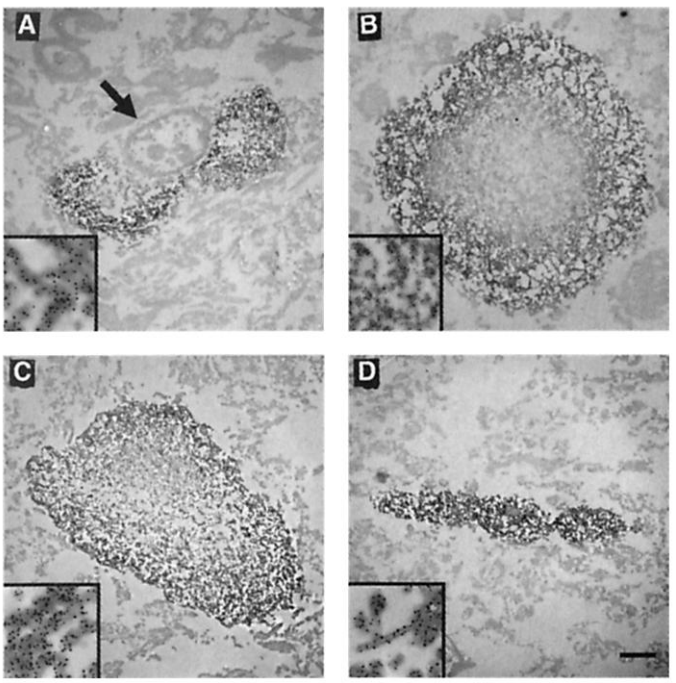

Fig. 4. Silver enhanced immunoelectron microscopy of synucleinopathy lesions with anti–nitrated α/β-syn mAb, nSyn 24. (**A**) Immunopositive GCI filaments in MSA. The arrow indicates the nucleus of the oligodendrocyte. Classical LB-like (**B**), spheroidlike (**C**), and LN-like (**D**) inclusions in NBIA 1. (**Insets**) Immunolabeled tubular, filamentous structures at higher magnification. The inset in (D) depicts a rare straight filamentous structure in spheroid and LN-like inclusions. Bar, 2 μm for low-magnification images and 200 nm for insets. Immunopositive structures visualized with DAB were silver-enhanced as described (*38*).

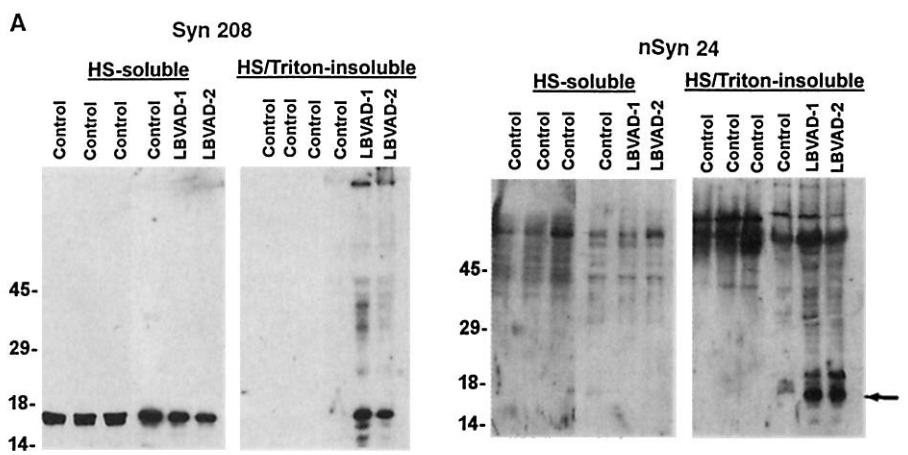

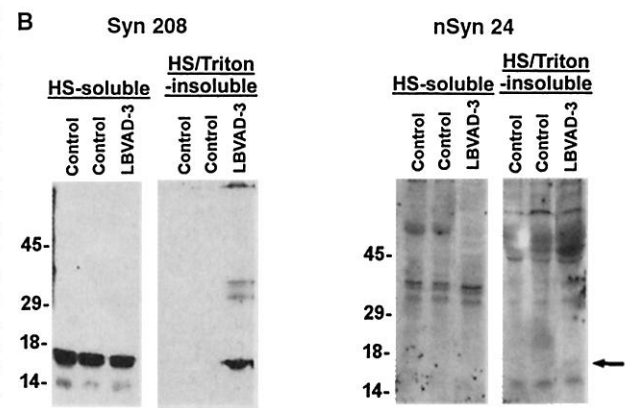

Fig. 5. Nitrated α-syn is in the HS/Triton-insoluble fraction of LBVAD brains. Gray-matter extracts of cingulate gyrus (**A**) or amygdala (**B**) from neuropathologically normal brain (control) or LBVAD brains were biochemically fractionated into HS/Triton-soluble and -insoluble fractions (*39*) followed by ECL-based Western blot analysis with anti–α-syn–specific antibody Syn 208 or anti–nitrated α/β-syn antibody nSyn 24 as probes. The arrow indicates the presence of nitrated α-syn in the HS/Triton-insoluble fraction of LBVAD brains. Higher molecular mass species detected by nSyn 24 mAb are nonspecific bands because they are present in both control and LBVAD samples.

References and Notes

1. W. R. Markesbery, J. M. Carney, *Brain Pathol.* **9**, 133 (1999).
2. P. Jenner, C. W. Olanow, *Neurology* **47**, S161 (1996).
3. P. Jenner, *Mov. Disord.* **13** (suppl. 1), 24 (1998).
4. L. Lyras *et al.*, *J. Neurochem.* **71**, 302 (1998).
5. M. R. Cookson, P. J. Shaw, *Brain Pathol.* **9**, 165 (1999).
6. S. E. Browne, R. J. Ferrante, M. F. Beal, *Brain Pathol.* **9**, 147 (1999).
7. C. R. White, R. P. Patel, V. Darley-Usmar, *Methods Enzymol.* **301**, 288 (1999).
8. V. B. O'Donnell *et al.*, *Chem. Res. Toxicol.* **12**, 83 (1999).
9. H. Ischiropoulos, *Arch. Biochem. Biophys.* **356**, 1 (1998).
10. A. Gow, D. Duran, S. R. Thom, H. Ischiropoulos, *Arch. Biochem. Biophys.* **333**, 42 (1996).
11. L. Maroteaux, J. T. Campanelli, R. H. Scheller, *J. Neurosci.* **8**, 2804 (1988).
12. J. M. George, H. Jin, W. S., Woods, D. F. Clayton, *Neuron* **15**, 361 (1995).
13. R. Jakes, M. G. Spillantini, M. Goedert, *FEBS Lett.* **345**, 27 (1994).
14. R. Kruger *et al.*, *Nature Genet.* **18**, 106 (1998).
15. M. H. Polymeropoulos *et al.*, *Science* **276**, 2045 (1997).
16. M. G. Spillantini *et al.*, *Nature* **388**, 839 (1997).
17. M. G. Spillantini, R. A. Crowther, R. Jakes, M. Hasegawa, M. Goedert, *Proc. Natl. Acad. Sci. U.S.A.* **95**, 6469 (1998).
18. M. Baba *et al.*, *Am. J. Pathol.* **152**, 879 (1998).
19. P. H. Tu *et al.*, *Ann. Neurol.* **44**, 415 (1998).
20. M. G. Spillantini *et al.*, *Neurosci. Lett.* **251**, 205 (1998).
21. S. Arawaka, Y. Saito, S. Murayama, H. Mori, *Neurology* **51**, 887 (1998).
22. P. F. Good, A. Hsu, P. Werner, D. P. Perl, C. W. Olanow, *J. Neuropathol. Exp. Neurol.* **57**, 338 (1998); J. E. Duda *et al.*, *Am J. Pathol.* **157**, 361 (2000).
23. Murine mAbs were raised against recombinant human α-syn nitrated in vitro as described (*28*). Briefly, nitrated α-syn (100 μg) emulsified in Freund's complete adjuvant was injected subcutaneously in BALB/c mice, followed by a subcutaneous injection of 25 μg of nitrated α-syn emulsified in Freund's in-

complete adjuvant on day 21 and an intravenous injection of 25 μg of nitrated α-syn in phosphate-buffered saline on day 48. On day 51, the spleen was removed and the lymphocytes were fused to myeloma cells (line Sp2/0-Ag14) by using polyethylene glycol 1500.
24. Y. Z. Ye, M. Strong, Z. Q. Huang, J. S. Beckman, *Methods Enzymol.* **269**, 201 (1996).
25. B. I. Giasson, unpublished observations.
26. C. F. Lippa, M. L. Schmidt, V. M.-Y. Lee, J. Q. Trojanowski, *Ann. Neurol.* **45**, 353 (1999).
27. J. E. Duda, unpublished observations.
28. B. I. Giasson *et al.*, *J. Neurosci. Res.* **59**, 528 (2000).
29. D. W. Dickson *et al.*, *Am. J. Pathol.* **155**, 1241 (1999).
30. B. I. Giasson *et al.*, unpublished observation.
31. J. M. Souza, B. I. Giasson, Q. Chen, V. M.-Y. Lee, H. Ischiropoulos, *J. Biol. Chem.* **275**, 18344 (2000).
32. M. A. Smith, P. L. Rickey Harris, L. M. Sayre, J. S. Beckman, G. Perry, *J. Neurosci.* **17**, 2653 (1997).
33. P. F. Good, P. Werner, A. Hsu, C. W. Olanow, D. P. Perl, *Am. J. Pathol.* **149**, 21 (1998).
34. M. L. Schmidt *et al.*, *Am. J. Pathol.* **139**, 53 (1991)
35. J. Q. Trojanowski, T. Schuck, M. L. Schmidt, V.M-Y. Lee, *J. Histochem. Cytochem.* **37**, 207 (1989).
36. B. I. Giasson, K. Uryu, J. Q. Trojanowski, V. M.-Y. Lee, *J. Biol. Chem.* **274**, 7619 (1999).
37. As described previously (*18*, *34*), blocks of cingulate cortex, hippocampus, and midbrain from postmortem DLB and LBVAD brians, as well as cerebellar white matter from MSA brains and globus pallidus from an NBIA1 brain, were immersion-fixed in 70% ethanol with 150 mM NaCl for 24 to 36 hours. The samples were dehydrated through a series of graded ethanol steps to xylene at room temperature and infiltrated with paraffin at 60°C as described (*35*) and then cut into multiple, near-serial 6-μm sections for immunohistochemistry by incubating the sections with primary antibody at 37°C for 90 min or at 25°C overnight followed by application of avidin-biotin complex (ABC) system (Vectastain ABC Elite Kit, Vector Laboratories, Burlingame, CA) and the chromagen 3,3′-diaminobenzidine (DAB) to visualize immunolabeled structures in sections lightly counterstained with hematoxylin.
38. E. M. Rodriguez, R. Yulis, B. Peruzzo, G. Alvial, R. Andrade, *Histochemistry* **81**, 253 (1984).
39. Gray matter (0.5 g) from the cingulate gyrus or the amygdala of LBVAD and control brains was dissociated with a Dounce homogenizer by using 10 ml of HS buffer [50 mM tris (pH 7.4), 750 mM NaCl, 10 mM NaF, 5 mM EDTA with protease inhibitors] per gram of tissue and sedimented at 100,000*g* for 30 min. The resulting pellets were reextracted with 10 ml of HS buffer–0.5 % Triton X-100 per gram of tissue. After centrifugation, the pellets were resuspended in 1.0 M sucrose–HS buffer and layered on a discontinuous 1.2 M/1.5 M/2.2 M sucrose gradient. After centrifugation at 200,000*g* for 2 hours, each fraction was assayed by Western blot analysis to determine the presence of α-syn. Most of the α-syn was located at the 1.5 M/2.2 M sucrose interphase (250 μl), and this fraction was used to assay for the presence of nitrated protein. Ten microliters of HS-soluble fractions and 1.5 M/2.2 M sucrose-interphase fractions, termed HS/Triton-insoluble, were loaded on separate lanes of 12% polyacrylamide gels for Western blot analysis.
40. We thank the Biochemical Imaging Core Facility of the University of Pennsylvania for assistance with the electron microscopy studies and the families of patients whose generosity made this research possible. Funded by grants from the National Institutes on Aging and by a Pioneer Award from the Alzheimer's Association. B.I.G. is the recipient of a fellowship from the Human Frontier Science Program Organization.

24 May 2000; accepted 20 September 2000

Role of *BAX* in the Apoptotic Response to Anticancer Agents

Lin Zhang, Jian Yu, Ben Ho Park, Kenneth W. Kinzler, Bert Vogelstein*

To assess the role of *BAX* in drug-induced apoptosis in human colorectal cancer cells, we generated cells that lack functional *BAX* genes. Such cells were partially resistant to the apoptotic effects of the chemotherapeutic agent 5-fluorouracil, but apoptosis was not abolished. In contrast, the absence of *BAX* completely abolished the apoptotic response to the chemopreventive agent sulindac and other nonsteroidal anti-inflammatory drugs (NSAIDs). NSAIDs inhibited the expression of the antiapoptotic protein Bcl-X_L, resulting in an altered ratio of BAX to Bcl-X_L and subsequent mitochondria-mediated cell death. These results establish an unambiguous role for *BAX* in apoptotic processes in human epithelial cancers and may have implications for cancer chemoprevention strategies.

The induction of apoptosis, or programmed cell death, in cancer cells is thought to be fundamental to the success of treatments for cancer. The *Bcl-2* family members are intimately involved in the apoptosis (*1*, *2*), but the role of these proteins in drug-induced death has been confusing. *BAX*, the prototypic death-promoting member of the *Bcl-2* family, provides a good example of the complications that have arisen. Many studies have relied on overexpression of BAX protein, conditions that may not faithfully reproduce its normal activity, and have yielded conflicting results (*3*). Drugs induce endogenous *BAX* expression through p53-dependent transcription in some cancer cell lines, but not others (*4*). In mice, *BAX* plays no role in the most well-studied examples of drug- or radiation-induced and p53-dependent apoptosis, involving thymocytes and intestinal epithelium (*5*–*7*). Unlike the human gene, the murine *BAX* gene has no p53-binding site in its promoter (*8*). Nevertheless, *BAX* deficiency promotes drug resistance in murine fibroblasts by partially attenuating p53-dependent apoptosis, but only when such cells are transformed with the adenoviral *E1A* oncogene (*3*, *9*). This picture is further confounded by the finding that *BAX* deficiency can promote rather than inhibit apoptosis in some murine cell types (*10*).

The most important targets of chemotherapeutic agents are human epithelial cells, which give rise to the vast majority of naturally occurring cancers. To clarify the role of *BAX* in drug-induced apoptosis in such cells, we created and studied isogenic derivatives that differ only in the presence or absence of the *BAX* gene. HCT116 colorectal cancer cells were chosen as the parental cells because they contain normal *p53* and *BAX* genes and undergo apoptosis in response to 5-fluorouracil (5-FU) and sulindac. 5-FU is the mainstay of treatment for colorectal cancer and is an antimetabolite that induces cell death in a p53-dependent manner (*11*). Sulindac is the prototypic chemopreventive agent for patients with colorectal cancer predisposition and is a nonsteroidal anti-inflammatory drug (NSAID) that binds to and inhibits cyclooxygenases and other cellular proteins (*12*–*14*).

To obtain isogenic cells differing in *BAX* status, we first exploited the innate propensity of mismatch repair (MMR)–deficient cells to mutate mononucleotide tracts (*15*). *BAX* contains an unstable G_8 tract at nucleotides 114 to 121 (codons 38 to 41) that is often mutated in MMR-deficient tumors (*16*). Through analysis of unselected subclones (*17*), we found that 2% of HCT116 cells had two intact *BAX* alleles, 94% had one intact allele (+/−, with one allele containing a deletion or insertion of a G within the G_8 tract), and 4% had two mutant alleles (−/− cells). Western blots confirmed the absence of BAX protein in the $BAX^{-/-}$ cells (Fig. 1A). In $BAX^{+/+}$ and $BAX^{+/-}$ cells, there was a slight induction of BAX protein by agents that activate p53 (Fig. 1A). Induction of p53 by 5-FU caused equivalent amounts of apoptosis in $BAX^{+/+}$ and heterozygous $BAX^{+/-}$ cells. The extent of apoptosis was somewhat reduced in the $BAX^{-/-}$ cells, but *BAX* deficiency did not recapitulate the effects of *p53* deficiency, which provided nearly complete protection against 5-FU–induced apoptosis (Fig. 1B) (*11*). In marked contrast, *BAX* deficiency completely eliminated the apoptosis induced by sulindac (Fig. 1B). In this case, *p53* deficiency had no effect, indicating that the apoptosis induced by sulindac was *p53*-independent. A similar effect of BAX deficiency was observed on the apoptosis in-

Howard Hughes Medical Institute, Oncology Center, and Program in Human Genetics, Johns Hopkins University School of Medicine, Baltimore, MD 21231, USA.

*To whom correspondence should be addressed. E-mail: vogelbe@welch.jhu.edu